Polarization fields of III-nitrides grown in different crystal orientations



2007 J. Phys.: Condens. Matter 19 403201

(http://iopscience.iop.org/0953-8984/19/40/403201)

IOP PUBLISHING JOURNAL OF PHYSICS: CONDENSED MATTER

J. Phys.: Condens. Matter **19** (2007) 403201 (26pp) doi:10.1088/0953-8984/19/40/403201

**TOPICAL REVIEW**

# Polarization fields of III-nitrides grown in different crystal orientations

**M Feneberg and K Thonke**

Institut für Halbleiterphysik, Universität Ulm, 89069 Ulm, Germany

E-mail: martin.feneberg@uni-ulm.de

Received 3 July 2007
Published 11 September 2007
Online at stacks.iop.org/JPhysCM/19/403201

**Abstract**

This article reviews the piezoelectric properties of III-nitrides with emphasis on GaN, InN, and their ternary alloys. After a short literature survey we concentrate on semipolar and nonpolar quantum wells grown on crystal planes other than the commonly used *c* plane ({0001}). The electrostatic field within a quantum well causes a quantum confined Stark effect and thus lowers the radiative transition probability as well as the transition energy. The basic impact of the quantum confined Stark effect on the optical properties of GaInN/GaN quantum wells is discussed in detail. Some routes to determine the magnitude of the electric field are described, and recent results are considered. The measured values are compared to published piezoelectric tensor elements.

## Contents



  

## 1. Introduction

Blue and even green semiconductor light emitting diodes are now readily commercially available. But still these devices are expensive and only produced by few companies throughout the world. The quantum efficiency of such devices—typically based on nitrides—is very low compared to their red or yellow counterparts made from the arsenide or phosphide material system. Therefore, numerous recent scientific work deals with nonpolar and semipolar light emitting devices made from wurtzite nitride semiconductors. Growth on nonpolar or semipolar planes is a possible way to increase the quantum efficiency of blue and green nitride based light emitting devices. In the usual growth direction, which is the [0001] direction or the so-called *c* direction, maximum electrostatic fields arise in the quantum wells. These fields are due to piezoelectric and spontaneous polarization and they decrease the efficiency by separating electron and hole wavefunctions as well as lowering the radiative transition energy.

If it is possible to orient the quantization direction of the quantum wells in crystal orientations other than those of the highest electrostatic fields, the influence of the polarity of the wurtzite crystal structure can be minimized, leading to higher quantum efficiencies. Because the piezoelectric polarization field is strain dependent, it increases with the lattice mismatch between the quantum well (active layer) and the barrier or substrate material. In a state-of-the-art GaInN/GaN light emitting diode this effect limits the available wavelength region. High indium incorporation into the quantum wells leads to longer wavelengths, but also increases the electrostatic field strength and therefore reduces the overlap integral of the wavefunctions dramatically. Electrostatic fields of the order of some MV $cm^{-1}$ can easily arise in light emitting diodes emitting in the blue to green wavelength region. Avoiding these internal fields would allow the production of light emitting GaInN/GaN devices, especially lasers, for the green spectral region or with even lower transition energy since the ternary material $Ga_xIn_{1-x}N$ can be used theoretically to cover the whole visible wavelength range.

The scientific work on gallium nitride and its alloys with aluminium and indium started its most active phase after the development of the first blue light emitting diode [1] in the late 1990s. The early works were nearly all dedicated to GaN grown along the [0001] direction which is easier to obtain by heteroepitaxy on sapphire or SiC than in any other growth direction. Only in very recent years has work on nonpolar and semipolar nitride materials begun. The material quality of layers grown in non-*c* directions still cannot compete with that of *c*-plane GaN. But very recently proof-of-principle experiments showed electrically pumped lasers of nonpolar [2, 3] and even semipolar [4] devices opening up the route to increased device performance and new applications based on this successful material system.

This work summarizes some of the recent developments of nonpolar and especially semipolar GaN based semiconductors from a physicist's point of view. Therefore we neither concentrate on growth of unusual crystal orientations nor on processing of more efficient light emitting devices, but we want to discuss the fundamental physical properties of semipolar quantum wells that are dependent on the actual material parameters, which are strain situation, spontaneous and piezoelectric polarization fields, and radiative transition energy. Some experimental methods for determining the actual size of the field strength are described before a short summary is given.

## 2. Polarization

Nearly all commercially available GaInN based devices are grown on the {0001} plane (*c* plane), accepting huge piezoelectric fields due to lattice mismatch induced strain. For optoelectronic applications there already exist alternatives with reduced or even without

**Table 1.** Some spontaneous polarization coefficients reported in the literature in chronological order.

| $p^{sp}$ (C m$^{-2}$) | | | GaN | InN | AlN |
|---|---|---|---|---|---|
| Nardelli *et al* | [15] | Theory | −0.045 | | −0.123 |
| Bernardini *et al* | [14] | Theory | −0.029 | −0.032 | −0.081 |
| Bechstedt *et al* | [16] | Theory | −0.074 | −0.050 | −0.120 |
| Vurgaftman and Meyer | [10] | Review | −0.034 | −0.042 | −0.090 |

piezoelectric fields. Such crystal planes are called semipolar or nonpolar planes. While the planes perpendicular to the *c* plane like the $\{1\bar{1}00\}$ plane (*m* plane) and the $\{11\bar{2}0\}$ plane (*a* plane) of wurtzite GaN are completely nonpolar, any plane having a tilt angle between 0° and 90° relative to the [0001] direction is a semipolar plane by definition. Some of these semipolar crystal planes exhibit stable surfaces during growth, therefore being available not only for theoretical investigations. The most important ones are the $\{11\bar{2}2\}$ [5] and the $\{1\bar{1}01\}$ planes [6, 7] of GaN, both commonly observed as side facets during the first steps of epitaxial lateral overgrowth. Other semipolar planes are reported after growth on unusual substrate materials like the $\{1\bar{1}03\}$ planes developing on {110}-oriented $MgAl_2O_4$ (spinel) [8] or on $\{11\bar{2}0\}$-plane sapphire [9]. For spontaneous polarization fields only the tilt angle of the respective plane relative to the {0001} plane is of interest, while for determining the piezoelectric polarization fields the strain situation of the tilted pseudomorphically grown active layers is important. In this section we want to discuss the angle-dependent polarization fields.

An important issue is to distinguish between unit cell direction and crystal termination. When talking about polarization fields, only the unit cell direction is of importance, which is defined from the nitrogen towards the metal ion of the double layer of the hexagonal unit cell. The crystal termination, which can be an atomic nitrogen or more commonly an atomic metal layer alone, does not change the polarization direction. Even a nitrogen terminated layer can have its positive unit cell direction towards the termination layer and therefore the same polarization field direction as a metal terminated layer with the same unit cell direction.

### *2.1. Spontaneous polarization*

Spontaneous polarization is an intrinsic material property of wurtzite semiconductors. Due to the partially ionic nature of the bonds in III-nitrides between nitrogen and metal ions a polarization vector can be defined. This polarization does not vanish after summation over all single bonds due to differences in the bond lengths.

In an unstrained quantum well only the differences between the spontaneous polarization vectors of barrier and well materials lead to electrostatic fields and therefore to a change in the band structure. For InN and GaN the spontaneous polarization coefficients are almost equal. All ternary GaInN compounds therefore show even smaller spontaneous polarization fields than pure InN grown directly on GaN would have. A short numerical example will be given for an example *c*-plane GaInN quantum well on GaN with 10% indium content. The spontaneous polarization coefficients of InN and GaN are $p^{sp} = -0.042$ C m$^{-2}$ and $-0.034$ C m$^{-2}$, respectively (see in table 1 the values taken from [10]). Therefore, the $Ga_{0.9}In_{0.1}N$ layer has a spontaneous polarization coefficient of $-0.0348$ C m$^{-2}$, interpolated linearly. The resulting difference of the coefficients of barrier and well materials is 0.0008 C m$^{-2}$, assuming surrounding GaN barriers. Finally, the electrostatic field inside the quantum well is calculated by

$$\vec{P}^{sp} = \frac{p^{sp}}{\epsilon_0 \epsilon}\,\hat{z}. \tag{2.1}$$

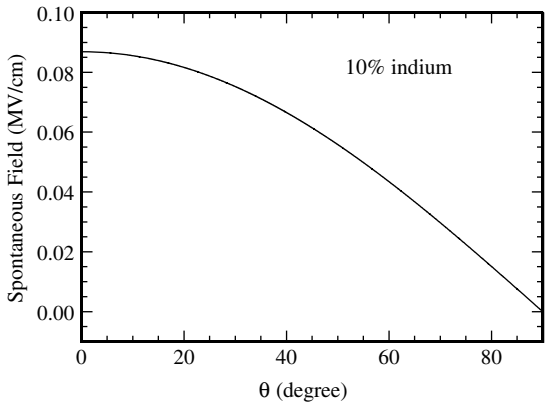


**Figure 1.** Spontaneous polarization field as function of the growth direction for a GaInN/GaN quantum well containing 10% indium. The field strength is calculated with the spontaneous polarization coefficients published in [10].

Here, $P^{\mathrm{sp}}$ is the electrostatic field due to spontaneous polarization, $p^{\mathrm{sp}}$ is the spontaneous polarization coefficient as described above, $\epsilon$ the dielectric constant of the material for which the field is calculated, $\epsilon_0$ the electrostatic dielectric constant, and $\hat{z}$ is the unit vector along the positive $c$-axis of the hexagonal crystal. One obtains for the field component in the $z'$ direction $F_z = 0.087\ \mathrm{MV\ cm^{-1}}$ using $\epsilon_{\|} = 10.4$. The positive sign of this value means that the field is oriented in the positive $z$ direction, which commonly in devices is the growth direction oriented from the substrate to the surface. If the growth direction does not match the $c$-axis of the hexagonal semiconductor, the remaining field strength in the quantization direction is the projection of this value on the off-axis growth direction following a simple cosine law (figure 1).

Compared to the field strengths resulting from piezoelectricity (compare section 2.4) the spontaneous polarization can be neglected for the GaInN/GaN material system without introducing any significant error. But for GaN/AlGaN quantum wells the situation is much more complicated. The spontaneous polarization coefficient for AlN is much larger ($-0.090\ \mathrm{C\ m^{-2}}$ [10]) than that for GaN, leading to comparable contributions to the overall electrostatic field by the spontaneous and by the piezoelectric components. We have to be aware of the fact that the spontaneous polarization coefficients for ternary alloys cannot be interpolated linearly, but are subject to a large bowing factor [11, 12]. If the spontaneous polarization field were the only contributing electrostatic field, it would be necessary to calculate its exact value for ternary GaInN on GaN. But for estimating the order of magnitude of its contribution relative to the electrostatic field, linear interpolation yields valid results and is much more conveniently performed. This is even more so because the bowing factor of the spontaneous polarization is still under discussion, and only very few results have been published yet. The growth angle dependence of the spontaneous polarization field of a GaN quantum well between AlGaN barriers with 10% aluminium content is shown in figure 2. Note that in this case the spontaneous polarization field is oriented along the negative $z'$ direction, meaning that the field points from the surface towards the substrate.

For comparison and completeness some frequently used spontaneous polarization coefficients reported in the literature are reproduced in table 1. Note that a measurement of only spontaneous polarization is very difficult. The only easily accessible candidate for such an investigation would be an unstrained AlInN/GaN quantum well, otherwise quantum wells of different composition would have to be compared carefully. We are aware of only

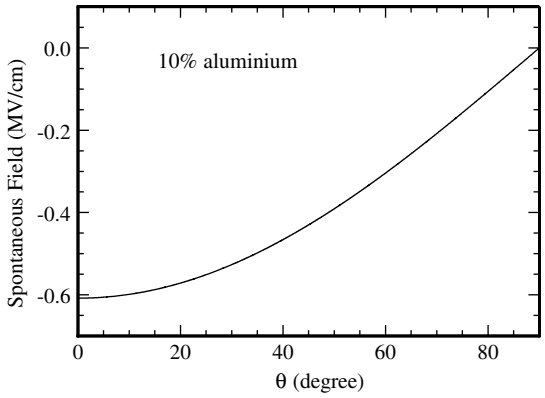


**Figure 2.** Spontaneous polarization field as a function of the growth direction for a GaN/AlGaN quantum well with barriers containing 10% aluminium. The field strength is calculated with spontaneous polarization coefficients published in [10].

one example in the literature [13] which confirms the spontaneous polarization coefficients published by Bernardini *et al* [14]. An electrostatic field present in such a quantum well should most probably arise only from spontaneous polarization, since the in-plane strain is low. The data available for the spontaneous polarization coefficients are therefore obtained theoretically.

### *2.2. Calculation of piezoelectric fields*

For a calculation of piezoelectric fields in wurtzite semiconductors, either the piezoelectric tensor **e** or the piezoelectric modulus **d** must be known. Both are linked by the elastic tensor **C** of the respective material

$$\mathbf{e} = \mathbf{d}\,\mathbf{C}. \tag{2.2}$$

More precisely, the piezoelectric tensor and piezoelectric modulus are tensors of third order. In Voigt's abbreviated notation they can be written as matrices like the elastic tensor:

$$\mathbf{e} = \begin{pmatrix} 0 & 0 & 0 & 0 & e_{15} & 0 \\ 0 & 0 & 0 & e_{15} & 0 & 0 \\ e_{31} & e_{31} & e_{33} & 0 & 0 & 0 \end{pmatrix}$$

$$\mathbf{d} = \begin{pmatrix} 0 & 0 & 0 & 0 & d_{15} & 0 \\ 0 & 0 & 0 & d_{15} & 0 & 0 \\ d_{31} & d_{31} & d_{33} & 0 & 0 & 0 \end{pmatrix}$$

$$\mathbf{C} = \begin{pmatrix} C_{11} & C_{12} & C_{13} & 0 & 0 & 0 \\ C_{12} & C_{22} & C_{13} & 0 & 0 & 0 \\ C_{13} & C_{13} & C_{33} & 0 & 0 & 0 \\ 0 & 0 & 0 & C_{44} & 0 & 0 \\ 0 & 0 & 0 & 0 & C_{44} & 0 \\ 0 & 0 & 0 & 0 & 0 & \frac{1}{2}(C_{11} - C_{12}) \end{pmatrix}.$$

The piezoelectric field $\vec{P}^{\mathrm{pz}}$ itself is the tensor product of the piezoelectric tensor or modulus and strain $\epsilon$ or stress tensor $\sigma$, respectively.

$$\vec{P}^{\mathrm{pz}} = \mathbf{e}\,\epsilon \tag{2.3}$$

$$\vec{P}^{\mathrm{pz}} = \mathbf{d}\,\sigma. \tag{2.4}$$

In this work we will only use the piezoelectric tensor **e** to simplify notation. If in any article cited the piezoelectric modulus **d** is given, we transform it into the piezoelectric tensor by using the elastic tensors which are reported by Vurgaftman and Meyer [10] for all III-N semiconductors. These values are widely accepted in the literature. The relevant relations are therefore

$$e_{31} = d_{31}(C_{11} + C_{12}) + d_{33}C_{13} \tag{2.5}$$

$$e_{33} = d_{31}2C_{13} + d_{33}C_{33} \tag{2.6}$$

$$e_{15} = d_{15}C_{44}. \tag{2.7}$$

For a calculation of $e_{31}$ or $e_{33}$ both $d_{31}$ and $d_{33}$ must be known, while $e_{15}$ only depends on $d_{15}$. If in a reference only one value of the piezoelectric modulus is reported, we estimate the corresponding value by using $d_{33} = -2\,d_{31}$ [17], which is legitimate as an approximation by comparison with other reported values.

Equation (2.3) can be written in Voigt's notation as

$$\vec{P}^{\mathrm{pz}} = \begin{pmatrix} 0 & 0 & 0 & 0 & e_{15} & 0 \\ 0 & 0 & 0 & e_{15} & 0 & 0 \\ e_{31} & e_{31} & e_{33} & 0 & 0 & 0 \end{pmatrix} \begin{pmatrix} \epsilon_1 \\ \epsilon_2 \\ \epsilon_3 \\ \epsilon_4 \\ \epsilon_5 \\ \epsilon_6 \end{pmatrix}. \tag{2.8}$$

Only three independent elements of **e** have to be determined. In the case of growth along the $c$-axis of a wurtzite crystal, the piezoelectric polarization vector only has a component along the $z$ direction, which is independent of $e_{15}$. For this reason some early work on the topic did not pay much attention to the value of $e_{15}$. A common simplification was to determine $e_{31}$ and $e_{33}$ and then to assume that $e_{15} = e_{31}$. In table 2 some reported values for the piezoelectric tensor components of GaN are reproduced. For InN the data base is less broad, while AlN has been investigated for decades. Quantum wells normally contain only a few per cent of indium or aluminium; therefore, measurements on such quantum wells usually confirm the piezoelectric tensor elements of GaN. Nevertheless, for calculations we interpolate linearly between the values of the binary semiconductors. Therefore, we reproduce also the values for InN (table 3) and some of those for AlN (table 4). Due to the fact that AlN is a classical material for surface acoustic wave (SAW) devices, the data reproduced here are far from being complete, since we concentrate mainly on GaN and GaInN.

A first look on the values reported for the piezoelectric tensor elements yields a wide scatter of parameters. A closer look especially on the values for GaN (table 2) shows that for $e_{31}$ and $e_{33}$ at least the sign and magnitude are reported consistently, while for $e_{15}$ only a few values are reported, scattered over a large range. The early value for $e_{15}$ [21] is less reliable because a simple assumption was made. With only the value for cubic GaN given ($e_{14} = 0.375$ C m$^{-2}$), it was assumed that $e_{31} = e_{15} = -1/\sqrt{3}e_{14}$ and $e_{33} = -2e_{31}$ hold. Both relations are empirically valid in some piezoelectric materials, but assuming $e_{15}$ equal to $e_{31}$ in GaN is an oversimplification. The value reported by Muensit *et al* [25] was experimentally determined and later approved theoretically by Bernardini and Fiorentini [30] and should be much more reliable. The sign of this value strongly influences the piezoelectric field strength for $\theta > 0$ and its value is essential in finding an eventually nonpolar plane with $\theta < 90°$. Our own recent measurement results also hint towards a positive value of $e_{15}$ [18].

The electrostatic field due to piezoelectric polarization is calculated similarly to that of the spontaneous polarization. But in this case the field may point in any direction, because $\vec{P}^{\mathrm{pz}}$ is a vector dependent on the strain tensor, while $\vec{P}^{\mathrm{sp}}$ is always parallel to the main symmetry axis

**Table 2.** Piezoelectric tensor elements for GaN from the literature in chronological order. If the reference gives values for the piezoelectric modulus only, the values have been transformed into piezoelectric tensor elements. If only one value of the piezoelectric modulus was given, we estimate the corresponding one by using $d_{33} = -2\,d_{31}$ [17] and mark the reference in the table with ⋆.

| GaN | (C m$^{-2}$) | $e_{31}$ | $e_{33}$ | $e_{15}$ | $e_{14}$ | |
|---|---|---|---|---|---|---|
| O'Clock and Duffy | [19] | | 1.24 | | | $k^2 = 0.04$ |
| Littlejohn *et al* | [20] | | | | 0.56 | |
| Bykhovski *et al* | [21] | −0.22 | 0.43 | −0.22 | 0.375 | Estimate from $e_{14}$ |
| Bernardini *et al* | [14] | −0.49 | 0.73 | | | |
| Muensit *et al* | [22] | −0.32 | 0.58 | | | **d** reported ⋆ |
| Takeuchi *et al* | [23] | −0.20 | 0.39 | (−0.35) | | |
| Shimada *et al* | [24] | −0.32 | 0.63 | −0.32 | 0.50 | |
| Guy *et al* | [17] | −0.55 | 1.12 | | | Bulk |
| Muensit *et al* | [25] | | | 0.33 | | **d** reported |
| Lueng *et al* | [26] | −0.53 | 0.89 | | | **d** reported ⋆ |
| Al-Yacoub and Bellaiche | [27] | −0.42 | 0.57 | | | |
| Bernardini *et al* | [28] | −0.37 | 0.67 | | | |
| Zorrodu *et al* | [29] | −0.37 | 0.67 | | | GGA values |
| | [29] | −0.47 | 0.86 | | | LDA values |
| Bernardini and Fiorentini | [30] | −0.46 | 0.78 | 0.19 | | **d** reported |
| Hangleiter *et al* | [31] | −0.31 | 0.56 | | | **d** reported ⋆ |
| Vurgaftman and Meyer | [10] | −0.53 | 0.89 | 0.33 | | **d** reported |
| Romanov *et al* | [32] | −0.49 | 0.73 | −0.40 | | |

**Table 3.** Piezoelectric tensor elements for InN from the literature in chronological order. If the reference gives values for the piezoelectric modulus only, the values have been transformed into piezoelectric tensor elements. If only one value of the piezoelectric modulus was given, we estimate the corresponding one by using $d_{33} = -2\,d_{31}$ [17] and mark the reference in the table with ⋆.

| InN | (C m$^{-2}$) | $e_{31}$ | $e_{33}$ | $e_{15}$ | |
|---|---|---|---|---|---|
| Bernardini *et al* | [14] | −0.57 | 0.97 | | |
| Al-Yacoub and Bellaiche | [27] | −0.59 | 0.95 | | |
| Takeuchi *et al* | [23] | −0.23 | 0.39 | | |
| Bernardini *et al* | [28] | −0.45 | 0.81 | | |
| Zorrodu *et al* | [29] | −0.45 | 0.81 | | GGA values |
| | [29] | −0.56 | 1.09 | | LDA values |
| Bernardini and Fiorentini | [30] | −0.48 | 1.06 | 0.26 | **d** reported |
| Cao *et al* | [33] | −0.48 | 0.82 | | **d** reported ⋆ |
| Hangleiter *et al* | [31] | −0.55 | 0.95 | | **d** reported ⋆ |
| Vurgaftman and Meyer | [10] | −0.48 | 1.06 | 0.26 | **d** reported |
| Romanov *et al* | [32] | −0.49 | 0.73 | −0.40 | |

of the hexagonal material.

$$\vec{F} = \frac{\vec{P}^{\mathrm{pz}}}{\epsilon_0 \epsilon}. \tag{2.9}$$

### *2.3. Strained layers*

To calculate the piezoelectric polarization field the strain $\epsilon$ must be known. First, the meaning of the six strain tensor elements in equation (2.8) must be clarified. According to Nye [38],

**Table 4.** Piezoelectric tensor elements for AlN from the literature in chronological order. If the reference gives values for the piezoelectric modulus only, the values have been transformed into piezoelectric tensor elements. If only one value of the piezoelectric modulus was given, we estimate the corresponding one by using $d_{33} = -2\,d_{31}$ [17] and mark the reference in the table with ⋆.

| AlN | (C m$^{-2}$) | $e_{31}$ | $e_{33}$ | $e_{15}$ | |
|---|---|---|---|---|---|
| Hutson | [34] | −0.53 | 1.43 | 0.46 | **d** reported |
| O'Clock and Duffy | [19] | | 1.94 | | $k^2 = 0.1$ |
| Tsubouchi *et al* | [35] | −0.58 | 1.55 | −0.48 | |
| Gualtieri *et al* | [36] | −0.58 | 1.55 | | |
| Kamiya *et al* | [37] | −0.72 | 1.92 | | **d** reported |
| Bernardini *et al* | [14] | −0.60 | 1.46 | | |
| Shimada *et al* | [24] | −0.38 | 1.29 | | $e_{14} = 0.59$ C m$^{-2}$ |
| Guy *et al* | [17] | −0.60 | 1.50 | | bulk |
| Muensit *et al* | [25] | | | 0.70 | **d** reported |
| Lueng *et al* | [26] | −0.81 | 1.35 | | **d** reported ⋆ |
| Bernardini *et al* | [28] | −0.62 | 1.50 | | |
| Zorrodu *et al* | [29] | −0.62 | 1.50 | | GGA values |
| | [29] | −0.74 | 1.80 | | LDA values |
| Bernardini and Fiorentini | [30] | −0.54 | 1.56 | 0.34 | **d** reported |
| Vurgaftman and Meyer | [10] | -0.54 | 1.56 | 0.42 | **d** reported |
| Romanov *et al* | [32] | −0.58 | 1.55 | −0.48 | |

their definition is

$$\begin{aligned}\epsilon_1 &= \epsilon_{xx}\\ \epsilon_2 &= \epsilon_{yy}\\ \epsilon_3 &= \epsilon_{zz}\\ \epsilon_4 &= 2\epsilon_{yz}\\ \epsilon_5 &= 2\epsilon_{xz}\\ \epsilon_6 &= 2\epsilon_{xy}.\end{aligned}$$

The $x$, $y$, and $z$ axes used throughout this article are defined according to figure 3. It is important to emphasize that the coordinate system $K$ is always oriented in the direction of the hexagon of the unit cell, while $K'$ is a coordinate system with its $z'$ direction perpendicular to the sample surface. Therefore the angle $\theta$ between $z$ and $z'$ gives the tilt angle of any unusual growth direction relative to the $c$-axis. This definition allows one to calculate straightforwardly the strain along any crystal direction in $K'$ coordinates and to transform the strain tensor back to $K$ coordinates, where equation (2.8) can be used. For wurtzite crystals this transformation is rotationally symmetric around the $z$ axis and only depends on the angle $\theta$, leading to

$$\begin{pmatrix} x' \\ y' \\ z' \end{pmatrix} = \begin{pmatrix} \cos\theta & 0 & -\sin\theta \\ 0 & 1 & 0 \\ \sin\theta & 0 & \cos\theta \end{pmatrix} \begin{pmatrix} x \\ y \\ z \end{pmatrix}. \tag{2.10}$$

The remaining task is to determine the strain components of an arbitrarily oriented crystal plane. Here, only pseudomorphically grown strained thin layers are discussed, e.g. quantum wells embedded in nominally unstrained barrier material. The calculation of strain in such layers has been the subject of different theoretical approaches. The calculation by Romanov *et al* [32] is very convenient to use due to explicit equations for the strain tensor components in all directions and in both coordinate systems. Another very sophisticated work has been published by Park and Chuang [39], who used a crystal energy minimization to obtain a complete set

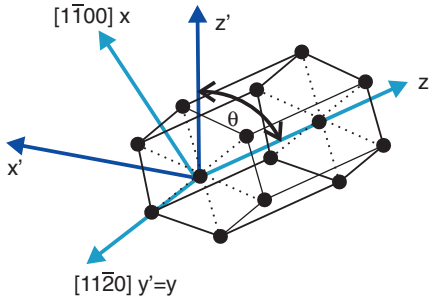


**Figure 3.** Sketch of the hexagonal crystal with the three Cartesian axes of the crystalline layer coordinate system $K$ and the substrate coordinate system $K'$ as described in the text.
(This figure is in colour only in the electronic version)

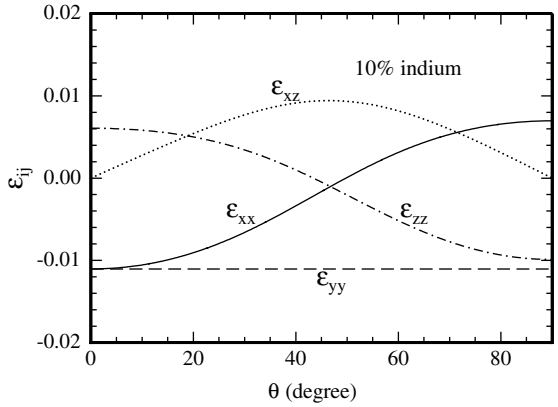


**Figure 4.** Strain components after Park and Chuang [39] as a function of the tilt angle for GaInN with 10% indium content.

of parameters. To test both methods again a GaInN layer with 10% indium is assumed to be pseudomorphically grown on unstrained GaN. The individual strain components as a function of the angle $\theta$ are plotted in figure 4 after Park and Chuang and in figure 5 after Romanov *et al* in the $K$ coordinate system. Only very minor differences are found despite the fact that the solution by Park and Chuang is only an approximation. All other strain components like $\epsilon_{xy}$ and $\epsilon_{yz}$ are equal to zero in the coordinate system chosen. Note that the coordinate system is defined differently in [32].

### *2.4. Piezoelectric fields*

The piezoelectric polarization vector $\vec{P}^{\mathrm{pz}}$ can now be calculated using equation (2.3), and the vector of the piezoelectric field follows from equation (2.9). Due to the fact that different values for the dielectric constants of the ternary alloy systems are reported in the literature, we compare the piezoelectric polarization and not the piezoelectric field strength calculated with different values for the piezoelectric tensor. The value of interest in this case is always the component of the piezoelectric polarization (or field) parallel to the quantization direction, i.e. normal to the surface. Therefore all piezoelectric polarization and field components are shown in $K'$ coordinates. For the calculation of fields we use in the following as dielectric

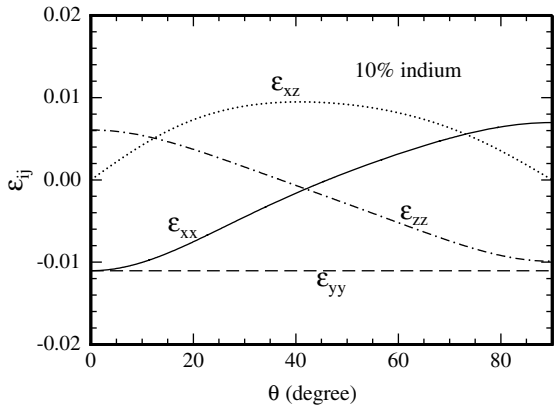


**Figure 5.** Strain components after Romanov *et al* [32] as a function of the tilt angle for GaInN with 10% indium content.

constants values linearly interpolated from the limiting binaries taken from [10]. For growth directions not parallel to the $z$ axis, one has to weight properly between the dielectric constants $\epsilon_\perp$ and $\epsilon_\parallel$, defined perpendicular and parallel to the $c$-axis, respectively.

As already mentioned, the piezoelectric polarization is dominated by the piezoelectric tensor elements of GaN (table 2) for quantum wells. Comparing the values reported in different references, we note that $e_{31}$ is negative, $e_{33}$ is positive, and $|e_{31}| < |e_{33}|$. For $e_{15}$ great differences are found: not even the sign is reported consistently. For the piezoelectric tensor elements of InN and AlN, basically the same statements hold. Calculation of the piezoelectric polarization as a function of the angle $\theta$ shows that the piezoelectric polarization always has its maximum for $\theta = 0°$, vanishes for growth on nonpolar planes ($\theta = 90°$), and may have an additional angle $0° < \theta < 90°$ with vanishing piezoelectric polarization. This specific angle depends on the exact value of the piezoelectric tensor components. Therefore, different angles for vanishing piezoelectric fields are obtained by different parameter sets. We have calculated the piezoelectric polarization as a function of the growth direction for the different parameter sets available for the piezoelectric tensor. Only those sets of tensor components are considered which also contain a value for $e_{15}$. If only a value for GaN is given in a reference, we interpolated linearly with the values reported by Vurgaftman and Meyer [10] for InN. This does not change the reported values much because the overall polarization is dominated by the values of GaN for low indium content. The calculations have been performed for different indium concentrations leading to different strain situations.

One complete set of values for the piezoelectric tensor elements is reported by Bykhovski *et al* [21]. They only report values for GaN; thus, values for InN from reference [10] were used for the linear interpolation. In figure 6 the piezoelectric polarization is shown for quantum wells grown in different directions with different indium concentrations. It can be seen that a nonpolar plane is obtained following the values of Bykhovski *et al* between $\theta_0 = 42°$ and 51°, dependent on the indium content. For $\theta > \theta_0$ the sign of the piezoelectric polarization changes as does therefore the piezoelectric polarization field.

Takeuchi and co-workers [23] published a curve for the angle dependence of the piezoelectric polarization field for a $Ga_{0.9}In_{0.1}N$ layer strained pseudomorphically on GaN. But they did not report the complete set of parameters of the piezoelectric tensor; only $e_{31}$ and $e_{33}$ were given. Therefore, we are not able to reproduce their curve exactly. After comparing curves for different $e_{15}$ with that of reference [23] we assume that Takeuchi *et al*

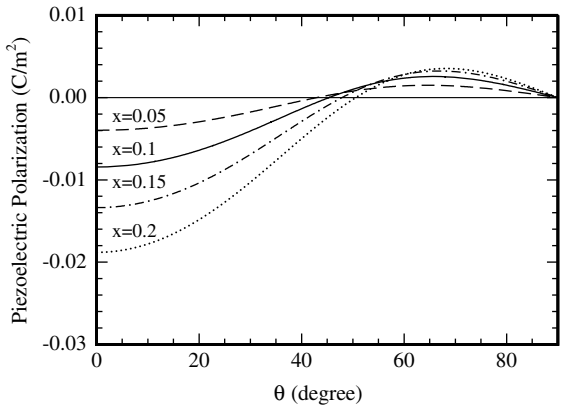


**Figure 6.** Piezoelectric polarization as a function of the growth direction for GaInN/GaN quantum wells, after Bykhovski *et al* [21]. The GaInN values have been linearly interpolated by using the InN values reported by Vurgaftman and Meyer [10].

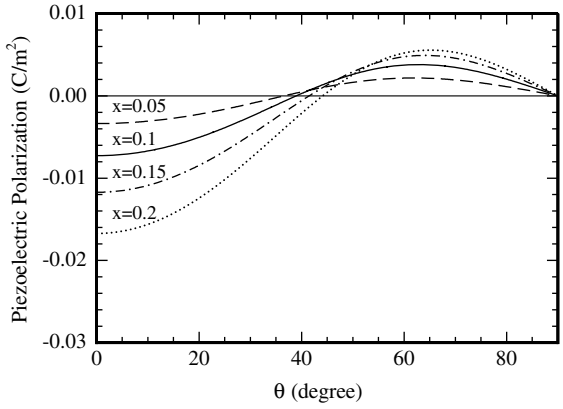


**Figure 7.** Piezoelectric polarization as a function of the growth direction for GaInN/GaN quantum wells. Calculated from values reported by Takeuchi *et al* [23].

used $e_{15} \approx -0.35$ C m$^{-2}$. The value for InN again does not play an important role. Calculated piezoelectric polarization curves with this value for $e_{15}$ for GaN, and $e_{15} = e_{31}$ for InN, are shown in figure 7.

For the polarization calculated with the values reported by Shimada *et al* [24] for GaN and again the Vurgaftman and Meyer [10] values for InN, the situation is very similar (figure 8) to that reported above. A polarization of zero is found between $\theta_0 = 42°$ and 48°. The size of the piezoelectric polarization is smaller compared to that of Bykhovski *et al* in figure 6. Note that, for both parameter sets, [21] and [24], the assumption $e_{31} = e_{15}$ has been used, and therefore $e_{15} < 0$ results.

Guy and co-workers [17, 25] published experimental results for all piezoelectric tensor elements. They found $e_{15} > 0$, which has the consequence that no intermediate angle $\theta_0$ exists with vanishing piezoelectric field (figure 9). The sign of the piezoelectric polarization and also of the piezoelectric field remains negative over the whole range, monotonically increasing from $\theta = 0°$ to 90°, where it vanishes. The experimental determination of $e_{15}$ should at least yield

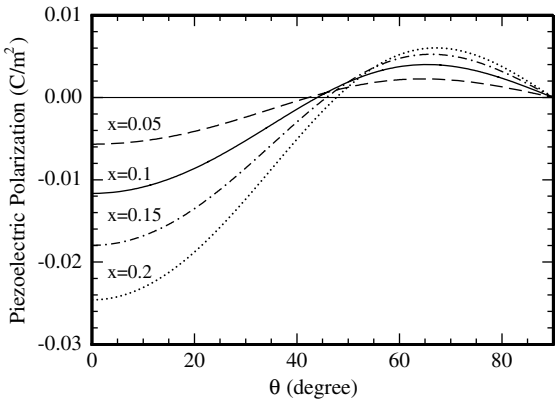


**Figure 8.** Piezoelectric polarization as a function of the growth direction for GaInN/GaN quantum wells, after Shimada *et al* [24]. The GaInN values have been linearly interpolated by using the InN values reported by Vurgaftman and Meyer [10].

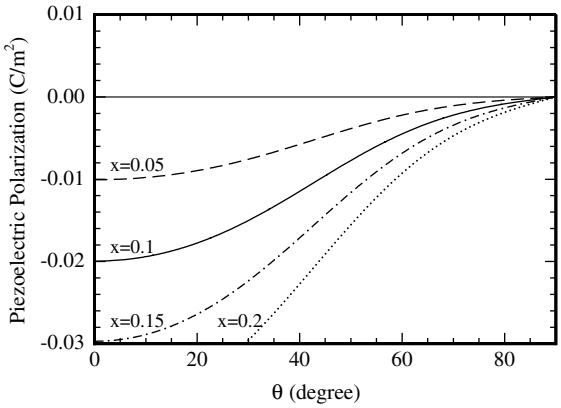


**Figure 9.** Piezoelectric polarization as a function of the growth direction for GaInN/GaN quantum wells, after Guy *et al* [17] and Muensit *et al* [25]. The GaInN values have been linearly interpolated by using the InN values reported by Vurgaftman and Meyer [10].

a more reliable sign than the assumption $e_{31} = e_{15}$ used before. We therefore consider the reported positive value of $e_{15}$ as more accurate than the negative one of earlier works.

Bernardini and Fiorentini [30] published values of the complete piezoelectric tensors for GaN, InN, and AlN. The values for InN reported by them are cited by Vurgaftman and Meyer in their review [10], because only a few values are available in the literature. Bernardini and Fiorentini derived their results by first-principles calculations and came up with positive values for $e_{15}$ for all three III-nitrides. (In fact they calculate positive $d_{15}$. With $C_{44} > 0$ it follows that $e_{15} > 0$; see equation (2.5).) The dependence of the piezoelectric polarization on $\theta$ is plotted in figure 10. Again, no nonpolar plane is found for $\theta < 90°$. The overall polarization strength is smaller than that calculated in figure 9.

Very recently, Romanov *et al* [32] published values for the piezoelectric tensor elements for GaN, InN, and AlN together with their strain calculations for arbitrarily grown pseudomorphic layers. For InN they used the same values as for GaN. The angle-dependent piezoelectric polarization calculated with these values has been already shown in [32]. For comparison, it

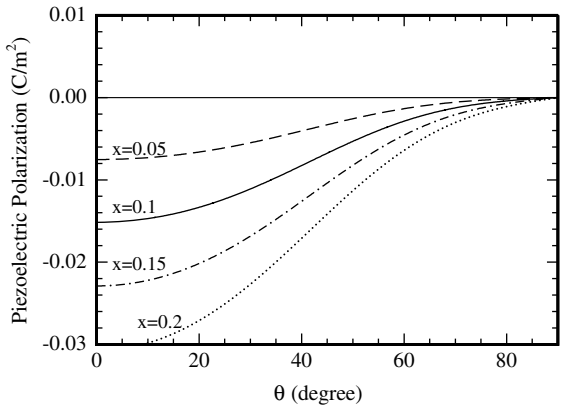


**Figure 10.** Piezoelectric polarization as a function of the growth direction for GaInN/GaN quantum wells, after Bernardini and Fiorentini [30]. The GaInN values have been linearly interpolated.

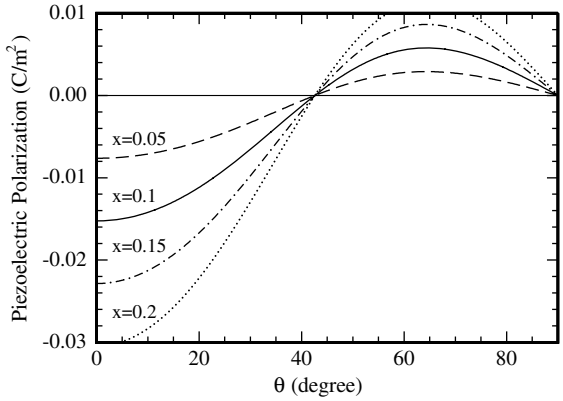


**Figure 11.** Piezoelectric polarization as a function of the growth direction for GaInN/GaN quantum wells, after Romanov *et al* [32]. For GaN and InN the same piezoelectric tensor is assumed; therefore, the differences for the different compositions only arise from the changed strain situation.

is reproduced here (figure 11) with the same axis scaling as before. A nonpolar plane around $\theta_0 = 42.5°$ is found for all indium compositions. The independence of $\theta_0$ on $x$ can be explained by the use of identical piezoelectric tensor elements both for InN and GaN. Therefore, the differences in the curves only arise from the differently strained layers, and not from any interpolation in piezoelectric tensor elements between GaN and InN.

### *2.5. Polarization fields*

The summation of both spontaneous and strain-induced polarization fields in GaInN/GaN quantum wells grown pseudomorphically yields the net polarization field. Rather different results are obtained for the different parameter sets of piezoelectric and spontaneous polarization constants. Parameters for piezoelectric and spontaneous polarization constants from different references are not necessarily comparable. Therefore, we use the constants reported by Bernardini and Fiorentini [30] and [14] for the piezoelectric and spontaneous

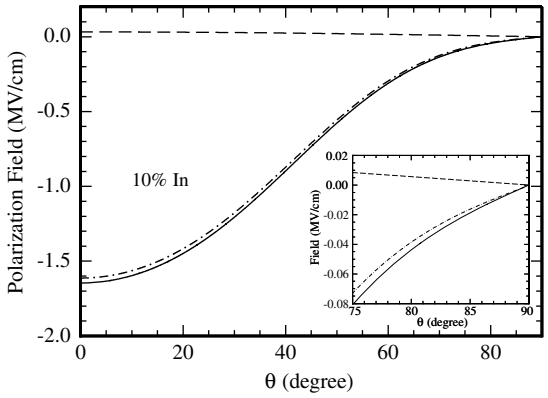


**Figure 12.** Net polarization field (dashed–dotted curve) composed of spontaneous polarization field (dashed curve) and piezoelectric polarization field (continuous curve) for a $Ga_{0.9}In_{0.1}N/GaN$ quantum well. The inset shows a magnification of the values for $\theta > 75°$ where the polarization field does not change its sign.

polarization constants, respectively. A quantum well containing 10% indium is assumed (matching the situation of figure 10). The values of the spontaneous polarization field are different from those of figure 1, because a different reference has been used there. The result is shown in figure 12 as a function of the growth angle $\theta$. Even after inclusion of the spontaneous polarization field having the opposite sign of the piezoelectric polarization field, the net electric field remains negative for all $\theta < 90°$. This is due to the fact that the absolute size of the spontaneous polarization field remains smaller than the piezoelectric polarization field for all angles. This remains true for all GaInN/GaN structures calculated with this parameter set, and again shows that in GaInN/GaN quantum wells the spontaneous polarization field can be neglected. The uncertainty coming from the differences in reported piezoelectric polarizations is much larger than the field due to spontaneous polarization.

## 3. Experimental determination of piezoelectric fields

### *3.1. SAW insertion-loss method*

In an SAW device the electromechanical coupling coefficient can be evaluated by insertion-loss measurements utilizing an equivalent circuit model. The value reported for the coupling coefficient, which can be written as $k$ or $k^2$, must be treated with caution. The relation between this value and the piezoelectric tensor element of the same direction is

$$k^2 = \frac{e_{33}^2/(C_{33}\epsilon_\parallel\epsilon_0)}{1 + e_{33}^2/(C_{33}\epsilon_\parallel\epsilon_0)} \tag{3.1}$$

if—as usual—the measurements have been performed along the ⟨0001⟩ direction. This is a mainly cubic dependence of $k^2$ on $e_{33}$, which is plotted in figure 13 for GaN with the values $C_{33} = 398$ GPa and $\epsilon_\parallel = 10.4$, where $\epsilon_\parallel$ is defined along the $z$-direction. Examples of this technique can be found in [19, 40]. A complete discussion of the reliability of insertion-loss measurements and its modelling by an equivalent circuit model is beyond the scope of this work. Most work of this type has been performed on AlN, but in [19] electromechanical coupling coefficients for GaN are reported which are of greater interest here. Two different values for $k^2$ measured along ⟨0001⟩ are given in [19] for different layer thickness. The higher

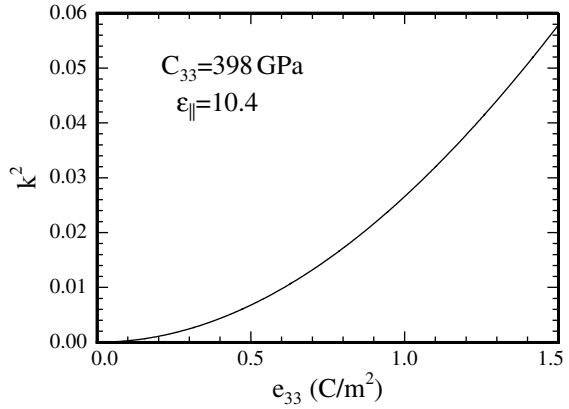


**Figure 13.** Electromechanical coupling coefficient $k^2$ oriented along the $c$-axis as a function of $e_{33}$.

one of both is measured in the thicker film (2 $\mu$m) and should be closer to the bulk value. It is reported to be $k^2 = 0.04$, which transforms following equation (3.1) to $e_{33} = 1.24$ C m$^{-2}$, as already noted in table 2. This value seems to be overestimated in comparison to the other values reported for $e_{33}$. For AlN the situation is very similar (see table 4); therefore, we think this overestimation probably comes from the equivalent circuit model which was used in the reference to derive $k^2$.

### *3.2. Interferometric experiments*

A rather direct method to measure the piezoelectric coefficients of GaN has been performed in [17, 22, 25, 26]. The piezoelectric material is subject to a high voltage applied on two contact pads and the material elongation or reduction is measured by a laser beam directed directly on the material or on an attached mirror in a Michelson interferometer. Depending on the crystal directions in which the voltage is applied and the elongation is measured, all piezoelectric constants—even $e_{15}$—can be measured separately. By comparing the results obtained it can be seen that the piezoelectric constants heavily depend on the material quality and type of material. Therefore, one has always to consider if the investigated material was polycrystalline or single-crystalline, grown on a template or free-standing. Most measurements performed so far have dealt with thin layers grown or sputtered on substrates. This is believed to influence the size of the piezoelectric coefficients heavily; for example, in a polycrystalline film grains with inverse unit cell orientation may occur, lowering the overall piezoelectric constant of the film. Therefore, despite the high quality of the sophisticated measurements, it is difficult to rate the different measured values or take one of them as valid generally.

### *3.3. Utilizing the quantum confined Stark effect*

The quantum confined Stark effect mainly reduces the transition probability between electron and hole states in a quantum well and also lowers its transition energy. Both effects can be used to determine the field strength. For the solutions of the quantum well Schrödinger equation we used the perturbation theory attempt published recently by Bulashevich *et al* [41], which we found quite accurate and very convenient to use. We checked the validity of this model by independent, self-consistent numerical solutions of the coupled Schrödinger and Poisson

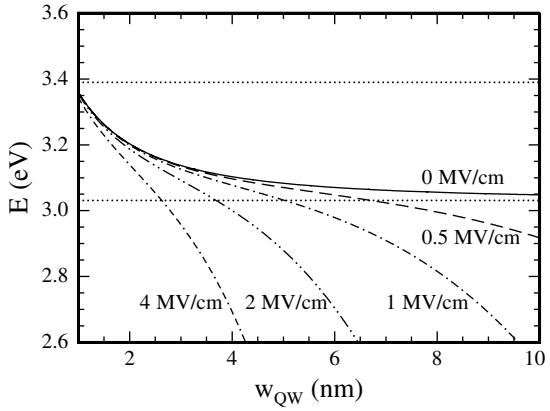


**Figure 14.** Transition energy of a *c*-plane GaInN/GaN quantum well containing 10% indium as a function of well width and piezoelectric field strength. The horizontal dotted lines denote the position of the bandgaps of GaN and bulk GaInN as used in the calculations.

equations. We found only minor deviations of the transition energies within a few per cent for all low-field cases, as is given for all quantum wells discussed here.

*3.3.1. Measuring the transition energy.* The focus of this work is polarization fields in quantum wells; therefore, all optical measurements allowing one to determine the field strength in quantum wells are of great interest here. Basically, only one single measurement of the optical transition energy of a well-known quantum well would be sufficient to determine the size (but not the direction) of the built-in field. This very simple experiment usually fails because the exact composition of the quantum well is in general not known. In GaInN, the indium concentration may furthermore fluctuate, and is difficult to determine quantitatively. Thus, it is better to vary a parameter and investigate the transition energy as a function of the varied parameter. As variable parameter it is convenient to use either well width, quantum well composition (e.g. indium concentration), excitation density, or externally applied voltage.

*Varying the quantum well width.* If the well width is varied at constant composition, the transition energy decreases with increasing width of the triangularly shaped finite quantum well. This quantum mechanical problem cannot be solved analytically, but numerical or perturbation theoretical solutions are readily available. Figure 14 shows the theoretical predictions for our example quantum well with 10% indium for different piezoelectric field strengths. No doping or screening effects are considered. The direction of the piezoelectric field cannot be obtained by this experiment. This method has been utilized, for example, in [31] to measure $d_{31}$ for *c*-axis oriented quantum wells.

*Varying the quantum well composition.* If the quantum well composition (in our case the indium concentration) is varied, the result is similar to the case where the quantum well width is varied. But the indium concentration is difficult to control while keeping the quantum well width constant simultaneously (and maintaining crystal quality). Furthermore, the effect is strongly dependent on the quantum well width. Note that the indium concentration is far more complicated to include in the calculations than the well width. The indium concentration $x$ affects of course the band gap of the quantum well, which is subject to a bowing parameter $b$,

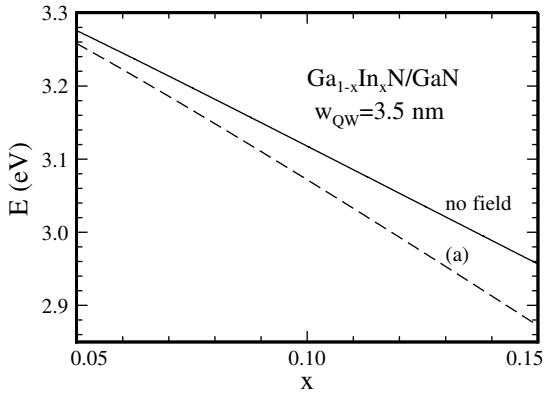


**Figure 15.** The dependence of the transition energy of a *c*-plane $Ga_{1-x}In_xN$/GaN quantum well with width $w_{QW} = 3.5$ nm on the indium content $x$. The situation is shown for a *c*-plane quantum well without piezoelectric field (no field) and one with piezoelectric field (a) using $e_{31}$ and $e_{33}$ by Bernardini and Fiorentini [30] for GaN and InN.

for which we use $b = 1$ eV in the following. Next, the quantization is weakly dependent on $x$, because the effective masses of GaN and InN have to be interpolated, which we neglect here. The strain situation is strongly dependent on the indium concentration $x$ being the driving force for piezoelectricity and finally, the material constants of the piezoelectric tensor and the elastic tensor must be known and interpolated between the values of the binaries. Mainly, the result is dominated by the values of pure GaN for quantum wells with some per cent indium, but one has to consider nonlinearities of $x$ carefully in a more general case. In figure 15 we show the results of calculations of the dependence on its composition of the transition energies of a 3.5 nm wide quantum well grown on the *c* plane of GaN. First, the indium dependence of the transition energy is shown without the inclusion of piezoelectric fields. Then, the piezoelectric tensor components of [30] are taken into account and the transition energy is calculated again. We chose [30] because there are values for both GaN and InN reported which are intermediate between those of table 2 and 3.

*Varying the excitation density.* The variation of excitation density varies the free carrier density in the quantum well, and therefore the piezoelectric field is screened with increasing excitation power. This experiment is easily performed and is often reported in the literature on different types of quantum well. But it is difficult to quantitatively interpret these experiments because the exact excitation power on the sample surface is already difficult to estimate due to unknown parameters like losses in optical components. The situation becomes even more complicated when absorption in a surface layer, especially the quantum well barrier, is considered. This can be circumvented by selective excitation below the bandgap of the barrier material. For our numerical example we chose again a GaInN/GaN quantum well with 10% indium and thickness 3.5 nm. The excitation power is taken into account as a two-dimensional free carrier density inside the quantum well. These free carriers are separated by the internal field, giving rise to a compensating electric field. In figure 16 the dependence of the transition energy on the free carrier density can be seen. If a critical carrier density is reached, the electric field in the quantum well is fully screened, which occurs in our example at about $n = 10^{12}$ cm$^{-2}$. For a higher piezoelectric field the unscreened transition energy decreases and therefore the overall shift increases. Our calculations shown in figure 16 do not take into

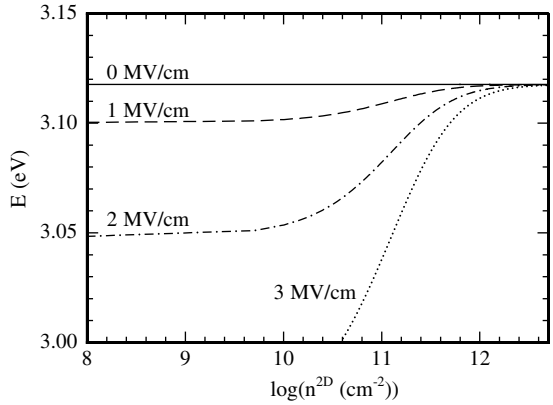


**Figure 16.** The dependence of the transition energy of a *c*-plane $Ga_{0.9}In_{0.1}N/GaN$ quantum well with width $w_{QW} = 3.5$ nm on the free carrier density inside the well.

account higher quantization states and band filling. Of course even in the case of vanishing piezoelectric polarization field high excitation should also lead to a blue shift of the transition energy, because at a certain excitation power the available states in the lowest band are filled up.

*Varying the externally applied voltage.* A further possibility to determine the piezoelectric field is to vary an externally applied voltage, which does directly influence the net internal field, and to measure at the same time the change in transition energy as observed by luminescence or absorption. This method is restricted to quantum wells embedded in a p/n diode structure, because otherwise high currents would probably destroy the quantum well or at least influence the result by carrier screening. Also it would not be easy to accurately calculate the fraction of the voltage drop across the quantum well and the barriers. In a diode, a backward voltage can be applied easily in a certain regime without destroying the device. The resistance of the whole structure is in any case dominated by the depletion region containing the quantum well. The potential across the barriers is tilted together with that of the quantum well, altering the tunnel rate and diminishing the luminescence intensity. The situation is shown schematically in figure 17. If—as is the case in *c*-plane GaInN/GaN quantum well diodes—the piezoelectric field points towards the substrate, and the p-doped region is the top layer, the flat-band situation can be reached at reverse voltages, yielding rather directly the size of the internal field. According to figure 17, a flat-band situation occurs for our standard example case for $U = -12$ V. The thin horizontal line marks the quantization energy level. Obviously, the transition energy increases with increasing backward voltage. The maximum transition energy therefore marks the flat-band point. One should further take into account the diffusion voltage or built-in voltage due to the different doping levels of the p and n regions. Already, without an applied external voltage, this leads to an additional term in the net internal field. A hypothetical quantum well with zero field would reach its flat-band condition when an external voltage that equals the built-in voltage is applied in the forward direction. For typical GaInN/GaN diodes the built-in voltage is about $V_{bi} \approx 3.3$ V. This information can be used to determine the sign of the internal piezoelectric field, because a negative field pointing towards the substrate would have its flat-band condition at a voltage lower than $V_{bi}$, while a positive piezoelectric field would presumably inhibit the observation of the flat-band point because an increased forward voltage would lead to high current and therefore to a high carrier density in

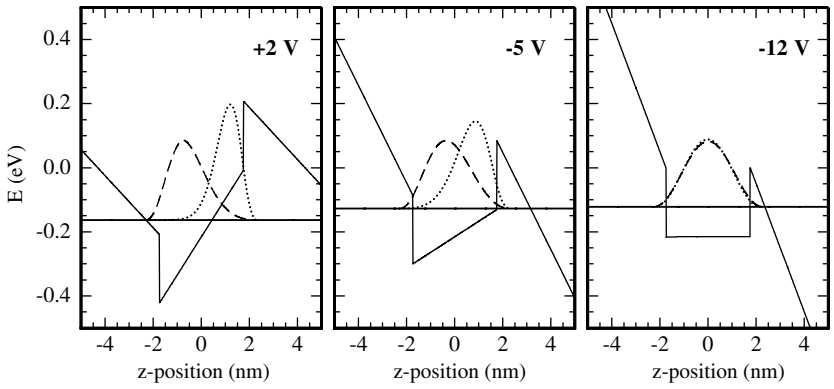


**Figure 17.** Conduction band profile of a GaInN/GaN quantum well embedded in a p/n diode shown schematically for different applied backward voltages. Flat-band situation occurs for approximately −12 V. Electron and hole wavefunctions are plotted dashed and dotted, respectively.

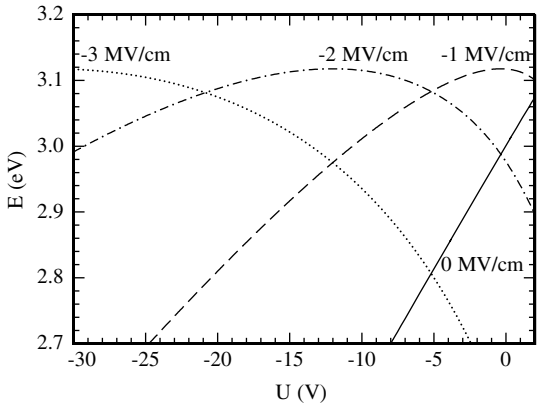


**Figure 18.** The dependence of the transition energy of a *c*-plane $Ga_{0.9}In_{0.1}N/GaN$ quantum well with width $w_{QW} = 3.5$ nm on the externally applied voltage. The quantum well is assumed between a n-doped region with $n = 5 \times 10^{18}$ cm$^{-3}$ and a p-doped region with $p = 7 \times 10^{17}$ cm$^{-3}$. Calculations are shown for different piezoelectric field strengths.

the quantum well. For the already well-introduced example $Ga_{0.9}In_{0.1}N/GaN$ quantum well with 3.5 nm thickness a numerical example is shown in figure 18. The quantum well in this case is embedded into a diode structure with p-doped and n-doped regions with active carrier densities of $p = 7 \times 10^{17}$ cm$^{-3}$ and $n = 5 \times 10^{18}$ cm$^{-3}$, respectively. The depletion region width as a function of voltage is take into account in the calculation. For the piezoelectric field strength different situations are shown. We find the flat-band situation of a realistic quantum well with a piezoelectric field of $-2$ MV cm$^{-1}$ to occur at about $V_a = -12$ V. The curve shape of the transition energy is asymmetric, because an increasing backward voltage also increases the width of the depletion region, while any positive voltage beyond $V_{bi}$ leads to a vanishing depletion zone width. Most interesting in this case is that the value of the flat-band voltage depends more or less on only the piezoelectric field strength. Therefore this method seems to be the most reliable one to measure the size and sign of the built-in piezoelectric field of GaInN/GaN quantum wells. Note that the transition energy at zero voltage is not equal to the

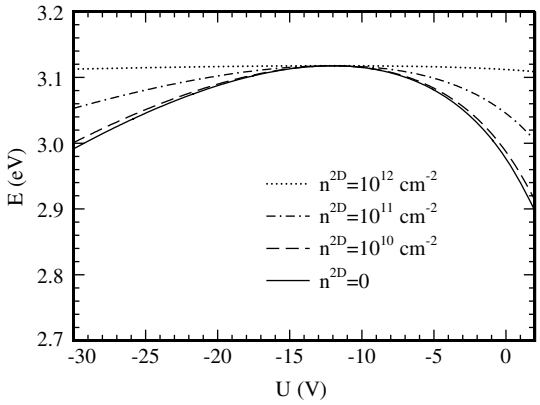


**Figure 19.** The dependence of the transition energy of a *c*-plane $Ga_{0.9}In_{0.1}N/GaN$ quantum well with width $w_{QW} = 3.5$ nm on the externally applied voltage. The piezoelectric field strength is assumed to be $-2$ MV cm$^{-1}$. The free carrier density is varied.

values reported before in this section, because here the quantum well is assumed to be placed in a depletion region. This leads to a net internal field $F$ of

$$F = \frac{V_{bi} - P^{pz}\, w_{QW} - V_a}{w_{QW} + d_d/2} + P^{pz}, \tag{3.2}$$

where $w_{QW}$ is the width of the quantum well, $V_a$ the externally applied voltage, and $d_d$ the width of the depletion region. Thus, besides the piezoelectric field, the built-in voltage and the applied voltage have to be taken into account. A piezoelectric field of $P^{pz} = -2$ MV cm$^{-1}$ after multiplication with $w_{QW} = 3.5$ nm leads to a corresponding voltage of $-0.7$ V, which is of the same order of magnitude as $V_{bi}$ and $V_a$. The same transition energy that can be found for the $-2$ MV cm$^{-1}$ case in figure 16 at low excitation is reached for an applied voltage of $V_a = -V_{bi}$. To perform this experiment under more realistic conditions one has to include the free carrier screening in the model calculation, too. This has been done in figure 19. This time, for a piezoelectric field strength of $-2$ MV cm$^{-1}$ the free carrier density has been varied as a parameter. Increasing the carrier density inside the quantum well flattens any transition energy shift caused by the quantum confined Stark effect due to screening effects. This is the reason why without a complete fit of the experimentally determined variation of the emission energy with the externally voltage applied (or in the best case the direct observation of the flat-band point) no certainty can be achieved in the determination of the piezoelectric field strength from only the magnitude of the shift. In particular, the estimate of piezoelectric field strength from the variation in transition energy only cannot yield reliable results, as long as the screening effect is not considered correctly.

Special attention in modelling a quantum well diode under reverse voltage should be paid to the correct calculation of the depletion region width. The depletion region broadens with increasing backward voltage. The technically relevant p-i-n diode, where the quantum wells are placed in an intrinsic region, is even more complicated. This problem was first addressed by Brown *et al* [42], who gave the width of the depletion region as a function of the applied voltage as

$$d_d = -d_u + \sqrt{d_u^2 + 2\left(\frac{N_D + N_A}{N_D\, N_A}\right)\frac{(V_{bi} - V_a)\epsilon\epsilon_0}{e}}. \tag{3.3}$$

Here, $d_u$ is the width of the intrinsic region, and $N_D$ and $N_A$ are the doping concentrations of n region and the p region, respectively.

*Experimental data for GaInN/GaN quantum wells in the literature.* Some reports can be found in the literature in which the size of the piezoelectric field of GaInN/GaN quantum wells is determined by this method. The results on *c*-plane GaInN/GaN quantum wells are summarized here.

The first report is by Takeuchi and co-workers [43]. They found a piezoelectric field of approximately $-1.2$ MV cm$^{-1}$ for a strained $Ga_{0.84}In_{0.16}N$/GaN quantum well after varying applied voltage and measuring photoluminescence simultaneously.

Brown *et al* [42] reinterpreted the data of Takeuchi *et al* [42] in terms of a new model considering a p-i-n diode instead of only a p/n diode. They reevaluate for the data of Takeuchi *et al* a piezoelectric field of $-2.6$ MV cm$^{-1}$. The measurements of Brown and co-workers themselves which are explained in the same reference yield a field of $-1.8$ MV cm$^{-1}$ for 10% indium content. These data have been derived by field-dependent absorption measurements.

Chichibu *et al* [44] performed photoluminescence measurements while varying the applied voltage. They find a piezoelectric field strength of $-1.4$ MV cm$^{-1}$ for an indium concentration of 25%. This value for the piezoelectric field seems to be very low, but the authors themselves explain that the indium content is only a rough estimate due to difficulties during x-ray measurements.

Renner and co-workers [45] analysed 11 quantum well samples with indium content between 7.4% and 9.2% and found piezoelectric fields between $-1.05$ and $-1.4$ MV cm$^{-1}$. They varied the externally applied voltage while measuring the absorption. Suspiciously, they did not find signatures of the quantum confined Stark effect but of the Franz–Keldysh effect, which usually occurs in bulk material.

Jho *et al* [46] also performed a field-dependent photoluminescence study in a very systematic way. They investigated samples containing 15% and 20% indium. In the case of the lower indium percentage they even observed the flat-band condition at $-22$ V resulting in a piezoelectric field of $-2.1$ MV cm$^{-1}$. The results on the sample with 20% indium remained unclear because the flat-band condition could not be found. Therefore, Jho *et al* claim the piezoelectric field to be very similar in magnitude.

Lai *et al* [47] performed bias-dependent electrotransmission experiments, which are basically a type of an absorption experiment as already described above. They find a piezoelectric field strength of about $-1.8$ MV cm$^{-1}$ for 23% indium. But their model implemented only a p/n diode, while they state in their sample description that it is in fact a p-i-n diode. Furthermore Lai *et al* claim to have grown quantum wells with 23% indium content, a statement based only on the growth parameters.

Franssen and co-workers [48] found a piezoelectric field of $-1.1$ MV cm$^{-1}$ for a quantum well with 8% indium by photocurrent spectroscopy. They used a reliable model and even discussed the influence of unavoidable band tail states on their spectra, but found no influence of the quantum confined Stark effect but again of the Franz–Keldysh effect, which may be a common property of quantum wells containing very low indium percentage.

Feneberg *et al* [18] also performed field-dependent photoluminescence experiments. The spectra are reproduced in figure 20. The analysis of the peak position is shown in figure 21, which after a full fit taking into account screening and built-in voltage yields a piezoelectric field of $-1.9$ MV cm$^{-1}$.

An overview of the published values of piezoelectric fields is shown in figure 22. We believe that the large scatter of the experimental results is caused by inaccuracies of the models used for analysis, primarily the use of a p/n diode model instead of a p-i-n diode model.

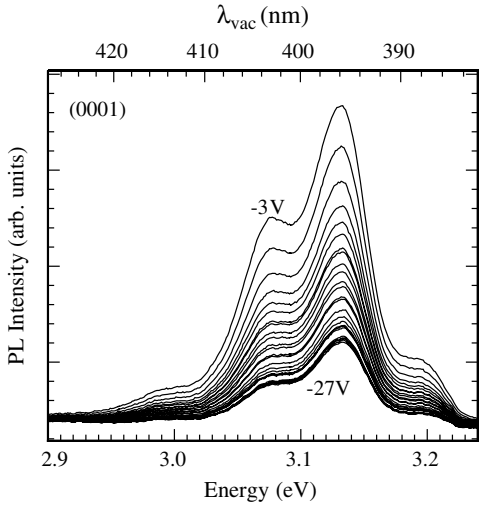


**Figure 20.** Photoluminescence spectra of a (0001) quantum well sample under reverse voltage.

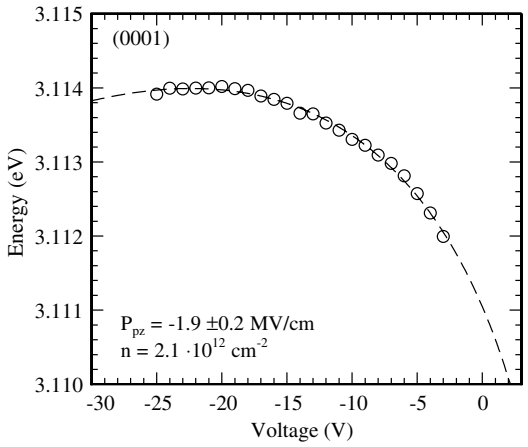


**Figure 21.** Peak positions of a (0001) sample as a function of applied voltage. The dashed curve is the fit to the data points yielding piezoelectric field and screening.

For semipolar GaInN/GaN quantum wells only one measurement of the piezoelectric field is found in the literature [18]. This experiment has been performed on the $\{1\bar{1}01\}$ side facets of selectively overgrown GaN stripes [49, 50]. On top of these stripes quantum wells with 15% indium content were grown. Here, the growth angle is $\theta = 62°$ relative to the $c$ direction. Field-dependent photoluminescence results are shown in figure 23. The voltage dependence of the peak positions yields a piezoelectric field of $-0.1$ MV cm$^{-1}$ in this case (figure 24). The flat-band condition is found at a voltage smaller than the built-in voltage, as discussed above. Therefore, the piezoelectric field is still negative for $\theta = 62°$. This findings fit well with the piezoelectric tensor elements reported by Bernardini and Fiorentini (see figure 12), however they are in contradiction with a possible nonpolar plane with $0° < \theta_0 \leqslant 62°$. A nonpolar plane for $62° < \theta_0 < 90°$ has never been suggested so far and therefore we conclude that it does not exist in GaN.

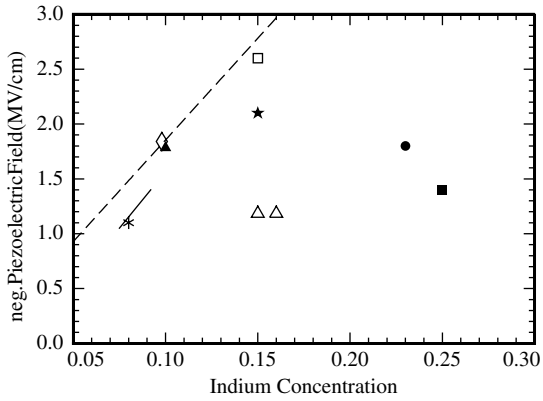


**Figure 22.** Dependence on the indium concentration of the values of piezoelectric field strengths reported in the literature for the different *c*-plane GaInN/GaN quantum wells shown. (▲) after Brown *et al* [42], (■) Chichibu *et al* [44], (line) Renner *et al* [45], (★) Jho *et al* [46], (●) Lai *et al* [47], (△) Takeuchi *et al* [43], (◇) Feneberg *et al* [18], and (∗) Franssen *et al* [48]. (□) denotes the values by Takeuchi *et al* [43] corrected by Brown *et al* [42]. For comparison the calculated piezoelectric field from the review of Vurgaftman and Meyer [10] is given as a dashed line.

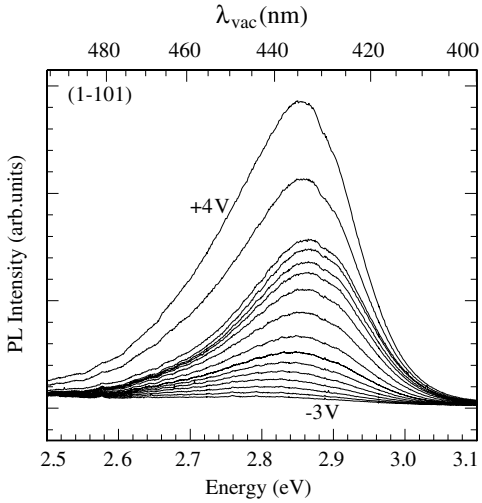


**Figure 23.** Photoluminescence spectra of a semipolar $\{1\bar{1}01\}$ multi-quantum well sample under reverse voltage.

*3.3.2. Measuring the transition probability.* Time-resolved photoluminescence can be used for the determination of the piezoelectric fields inside the quantum wells. The radiative decay time is inversely proportional to the transition matrix element. This matrix element is calculated as the overlap integral between the wavefunctions of electrons and holes. Therefore, a high piezoelectric field leads to strong separation of the wavefunctions, a low overlap integral and finally a long decay time. An advantage of this method to determine the piezoelectric fields experimentally is the rather direct measurement. The disadvantages are the large experimental effort for the time resolution needed and the calculative description of the results. Because the overlap integral of the wavefunctions is needed, a numerical computation is unavoidable in this case. Again, a parameter variation is necessary to overcome problems of not exactly known

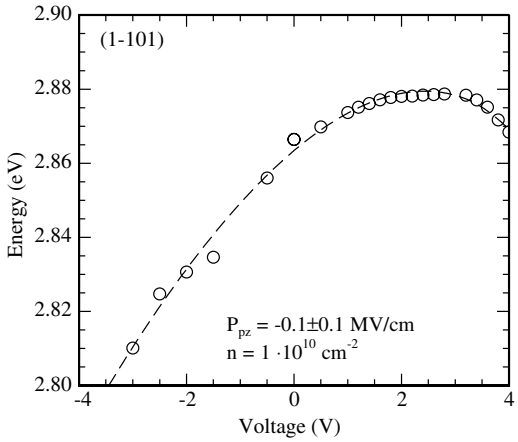


**Figure 24.** Peak positions of the semipolar sample as a function of applied voltage. The dashed curve is the fit to the data points yielding the piezoelectric field and screening.

material data to determine the piezoelectric field strength quantitatively. The parameters that can be varied are in principle the same as described above, with the difference that the measured quantity is the decay time instead of the transition energy.

## 4. Summary

This review addresses the polarization fields occurring in quantum wells of nitride semiconductors and their alloys. Spontaneous and piezoelectric polarization fields are explained and compared for different materials. A brief review is given over reported values for the spontaneous polarization coefficient and the piezoelectric tensor elements. The dependency of the polarization fields in quantum wells on the orientation of crystal planes ranging from the polar *c* plane to semipolar planes and the nonpolar *m* and *a* planes of wurtzite GaN has been discussed. Emphasis was laid on the influence of polarization fields on the optical properties of GaInN/GaN quantum wells, where the piezoelectric polarization dominates the net polarization. We have discussed and explained different techniques to determine the built-in electrostatic fields accurately and reviewed some of the work reported in the literature.

Our own measurements have been explained in detail and the findings have been compared to published values of polarization fields on different crystal planes. The most striking result is that the piezoelectric field is still negative for a growth angle of 62°, and therefore presumably for all angles. This result is in nearly perfect agreement with the values of the piezoelectric tensor elements published by Bernardini and Fiorentini [30] (or with those of Vurgaftman and Meyer [10]).

Very recently, the first GaInN/GaN laser diodes on nonpolar and semipolar crystal planes have been demonstrated. The near future will show if such devices will outperform *c*-plane based structures. Presumably, technological aspects will decide which crystal orientation turns out to be the most suitable for very demanding devices like green semiconductor laser diodes.

## Acknowledgments

The authors would like to thank Rolf Sauer (Institut für Halbleiterphysik, Universität Ulm) for steady support and encouragement. We thank Frank Lipski for measurements, and Peter

Brückner, Thomas Wunderer, and Ferdinand Scholz (Institut für Optoelektronik, Universität Ulm) for samples and many valuable discussions and experiments.

## References


[1] Nakamura S, Senoh M and Mukai T 1993 *Japan. J. Appl. Phys.* **32** L8
[2] Okamoto K, Ohta H, Chichibu S F, Ichihara J and Takasu H 2007 *Japan. J. Appl. Phys.* **46** L187
[3] Schmidt M C, Kim K C, Farrell R M, Feezell D F, Cohen D A, Saito M, Fujito K, Speck J S, DenBaars S P and Nakamura S 2007 *Japan. J. Appl. Phys.* **46** L190
[4] Tyagi A, Zhong H, Chung R B, Feezell DF, Saito M, Fujito K, Speck J S, DenBaars S P and Nakamura S 2007 *Japan. J. Appl. Phys.* **46** L444
[5] Beaumont B, Vaille M, Nataf G, Boillé A, Guillaume J C, Vénnègues P, Haffouz S and Gibart P 1998 *MRS Internet J. Nitride Semicond. Res.* **3** 20
[6] Kato Y, Kitamura S, Hiramatsu K and Sawaki N 1994 *J. Cryst. Growth* **144** 133
[7] Kapolnek D, Keller S, Vetury R, Underwood R D, Kozodoy P, DenBaars S P and Mishra U K 1997 *Appl. Phys. Lett.* **71** 1204
[8] Chakraborty A, Baker T J, Haskell B A, Wu F, Speck J S, DenBaars S P, Nakamura S and Mishra U K 2005 *Japan. J. Appl. Phys.* **44** L945
[9] Potin V, Vermaut P, Ruterana P and Nouet G 1998 *J. Electron. Mater.* **27** 266
[10] Vurgaftman I and Meyer J R 2003 *J. Appl. Phys.* **94** 3675
[11] Bernardini F and Fiorentini V 2001 *Phys. Rev.* B **64** 085207
[12] Fiorentini V, Bernardini F and Ambacher O 2001 *Appl. Phys. Lett.* **80** 1204
[13] Hsu T M, Lai C Y, Chang W H, Pan C C, Chuo C C and Chyi J I 2004 *Appl. Phys. Lett.* **84** 1114
[14] Bernardini F, Fiorentini V and Vanderbilt D 1997 *Phys. Rev.* B **56** R10024
[15] Nardelli M B, Rapcewicz K and Bernholc J 1997 *Phys. Rev.* B **55** R7323
[16] Bechstedt F, Grossner U and Furthmüller J 2000 *Phys. Rev.* B **62** 8003
[17] Guy I L, Muensit S and Goldys E M 1999 *Appl. Phys. Lett.* **75** 4133
[18] Feneberg M, Lipski F, Sauer R, Thonke K, Wunderer T, Neubert B, Brückner P and Scholz F 2006 *Appl. Phys. Lett.* **89** 242112
[19] O'Clock G D and Duffy M T 1973 *Appl. Phys. Lett.* **23** 55
[20] Littlejohn M A, Hauser J R and Glisson T H 1975 *Appl. Phys. Lett.* **26** 625
[21] Bykhovski A D, Kaminski V V, Shur M S, Chen Q C and Khan M A 1996 *Appl. Phys. Lett.* **68** 818
[22] Muensit S and Guy I L 1998 *Appl. Phys. Lett.* **72** 1896
[23] Takeuchi T, Amano H and Akasaki I 2000 *Japan. J. Appl. Phys.* **39** 413
[24] Shimada K, Sota T and Suzuki K 1998 *J. Appl. Phys.* **84** 4951
[25] Muensit S, Goldys E M and Guy I L 1999 *Appl. Phys. Lett.* **75** 3965
[26] Lueng C M, Chan H L W, Surya C and Choy C L 2000 *J. Appl. Phys.* **88** 5360
[27] Al-Yacoub A and Bellaiche L 2001 *Appl. Phys. Lett.* **79** 2166
[28] Bernardini F, Fiorentini V and Vanderbilt D 2001 *Phys. Rev.* B **63** 193201
[29] Zorrodu A, Bernardini F, Ruggerone P and Fiorentini V 2001 *Phys. Rev.* B **64** 045208
[30] Bernardini F and Fiorentini V 2002 *Appl. Phys. Lett.* **80** 4145
[31] Hangleiter A, Hitzel F, Lahmann S and Rossow U 2003 *Appl. Phys. Lett.* **83** 1169
[32] Romanov A E, Baker T J, Nakamura S and Speck J S 2006 *J. Appl. Phys.* **100** 023522
[33] Cao C B, Chan H L W and Choy C L 2003 *Thin Solid Films* **441** 287
[34] Hutson A R 1963 *US Patent Specification* 3090876
[35] Tsubouchi K and Mikoshiba N 1985 *IEEE Trans. Son. Ultrason.* **32** 634
[36] Gualtieri J G, Kosinski J A and Ballato A 1994 *IEEE Trans. Ultrason. Ferroelectr. Freq. Control* **41** 53
[37] Kamiya T 1996 *Japan. J. Appl. Phys.* **35** 4421
[38] Nye J F 1985 *Physical Properties of Crystals: Their Representation by Tensors and Matrices* (Oxford: Oxford University Press)
[39] Park S H and Chuang S L 1999 *Phys. Rev.* B **59** 4725
[40] Dubois M A and Muralt P 1999 *Appl. Phys. Lett.* **74** 3032
[41] Bulashevich K A, Karpov S Y and Suris R A 2006 *Phys. Status Solidi* b **243** 1625
[42] Brown I H, Pope I A, Smowton P M, Blood P, Thomson J D, Chow W W, Bour D P and Kneissl M 2005 *Appl. Phys. Lett.* **86** 131108
[43] Takeuchi T, Wetzel C, Yamaguchi S, Sakai H, Amano H, Akasaki I, Kaneko Y, Nakagawa S, Yamaoka Y and Yamada N 1998 *Appl. Phys. Lett.* **73** 1691

[44] Chichibu S F, Azuhata T, Sota T, Mukai T and Nakamura S 2000 *J. Appl. Phys.* **88** 5153
[45] Renner F, Kiesel P, Döhler G, Kneissl M, Van de Walle C and Johnson N 2002 *Appl. Phys. Lett.* **81** 490
[46] Jho Y D, Yahng J S, Oh E and Kim D S 2002 *Phys. Rev.* B **66** 035334
[47] Lai C Y, Hsu T M, Chang W H, Tseng K U, Lee C M, Chuo C C and Chyi J I 2002 *J. Appl. Phys.* **91** 531
[48] Franssen G, Perlin P and Suski T 2004 *Phys. Rev.* B **69** 045310
[49] Neubert B, Brückner P, Habel F, Scholz F, Riemann T, Christen J, Beer M and Zweck J 2005 *Appl. Phys. Lett.* **87** 182111
[50] Wunderer T, Brückner P, Neubert B, Scholz F, Feneberg M, Lipski F, Schirra M and Thonke K 2006 *Appl. Phys. Lett.* **89** 041121